AIAA 81-0237R

New Airborne Weather Radar Systems

G. A. Lucchi*
Sperry Flight Systems, Van Nuys, Calif.

This paper reviews the characteristics of airborne weather radars produced since World War II, citing the major technology changes that have been implemented up to the present time. The recent advent of large scale integrated (LSI) circuits has made it possible to design practical color radar displays which are more easily interpreted by the pilot. The paper reviews the weather radar range equation and then justifies the choice of radar parameters to permit the use of current state-of-the-art solid-state potentially reliable low-powered transmitters to provide adequate storm cell detection range. System parameter choices are considered for the use of a solid-state coherent radar system for extracting storm cell turbulence signals which can be of use in displaying their location to the pilot in order to avoid these potentially hazardous areas. It is concluded that this new technology airborne weather radar system will result in a more reliable radar which will also provide the pilot with sufficient navigation information to permit flying closer to large storm cells in areas free from turbulence, thus promoting passenger comfort and safety while conserving fuel.

Nomenclature

C = speed of light or radio propagation = 3×10^8 m/s
d = diameter of the storm cell in nautical miles = 3 n.mi.
G = antenna gain (one way) over isotropic expressed as a ratio
K = complex of refraction for water at the radar frequencies of interest. The absolute value of $|K|^2 = 0.93$ is commonly used
L = losses due to transmission line between R/T and antenna radiator, radome losses (these are two-way losses), system losses or gains for whatever cause can be justified, including intervening rain, and other atmospheric losses at the frequency of interest (this is a number)
P_r = received power at the radar R/T waveguide connector expressed in dB/m
P_t = W
r_a = unambiguous radar range = $CT_s/2$
T = transmitter pulse width in μs
T_s = pulse repetition time (PRT) or sample time interval
v_a = Nyquist velocity = $\lambda/4T_s$
Z = radar reflectivity factor (mm^6/m^3). It has a relationship to rainfall rate; however, a reflectivity factor of $Z = 10^5$ has been used for the storm model in the past
λ = radar carrier frequency wavelength for the particular frequency of interest. For C-band use 5.56 cm, for X-band use 3.2 cm, and for Ku-band use 1.9 cm as a reference
σ_v = velocity spectrum width of echos at range r

Current Weather Radar Designs

THE first air-carrier weather radar was flown by United Airlines during 1955. This C-band system developed a peak transmitter power of 75 kW, used a 2-μs pulse width and a 22-in.-diam parabolic antenna. Its maximum displayed range was 150 n.mi. This vacuum tube system weighed 125 lb, required 875 VA power from the aircraft's 115 V, 400 Hz supply, and consisted of five subsystems. The technology and many of the components used were of World War II vintage. This is shown in Fig. 1. Since this system would not fit in most general aviation aircraft, smaller X-band weather radar systems were made available by 1956 which developed a peak transmitter power of 40 kW, a 1.8-μs pulse width, a parabolic antenna as small as 12 in., requiring 515 VA of 115 V, 400 Hz primary power, weighed 63 lb, and consisted of four subassemblies. This system had a maximum range of 80 n.mi.

Air-carrier X-band weather radar systems became available during the early 1960s that generated peak transmitter powers of 40 kW, a 1.8-μs pulse width, a maximum range scale of 150 miles, a 30-in. parabolic antenna requiring at least 850 VA of 115 V, 400 Hz primary power, and a system weight of 149 lb for all of the five subsystems.

General aviation weather radar systems were being introduced at this time which produced a peak transmitter power of up to 25 kW, a 2-μs pulse width, antenna sizes up to 30 in. (most were 12 in.), a maximum display range of 180 n.mi., requiring only 250 VA of 115 V, 400 Hz power, and a three subsystem weight of 54 lb. This same radar system was being used by many regional and some overseas airlines. The new technology in these systems was the introduction of transistors, direct view storage tubes (DVST) for a slow fading display which could be viewed in direct sunlight, and for the first time, ferrite circulators and isolators. All of the airline radar systems employed some form of antenna stabilization using the aircraft vertical gyrosignals. This system is shown in Fig. 2.

It was not until the middle and late 1960s that weather radars were being offered to the general aviation user which required approximately 100 W of primary power, weighed

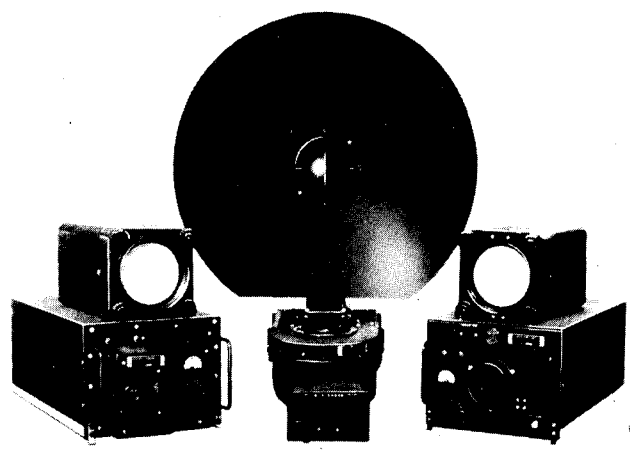

Fig. 1 RCA's AVQ-10 weather radar (C-band).

Presented as Paper 81-0237 at the AIAA 19th Aerospace Sciences Meeting, St. Louis, Mo., Jan. 12-15, 1981; submitted March 14, 1981; revision received June 23, 1981.

*Manager, Advanced Avionics Systems. Member AIAA.

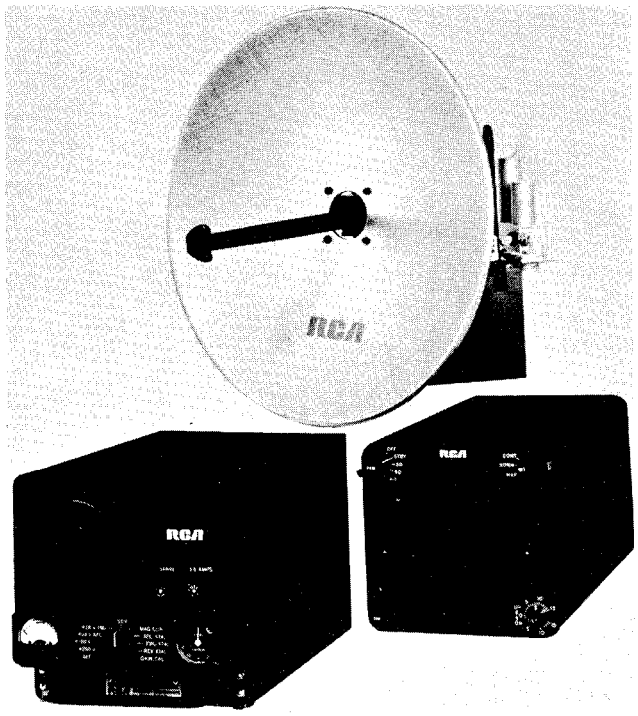

Fig. 2 RCA's AVQ-20A weather radar (X-band).

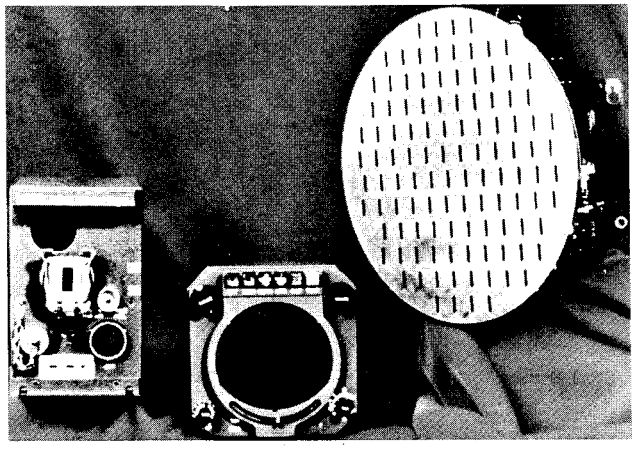

Fig. 3 RCA's AVQ-21 weather radar (X-band).

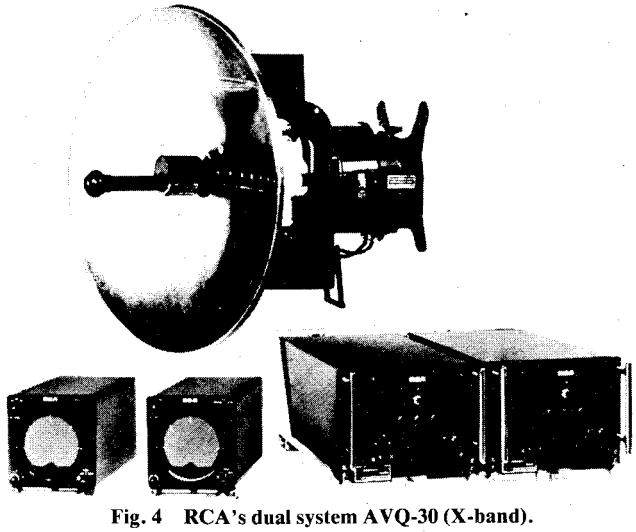

Fig. 4 RCA's dual system AVQ-30 (X-band).

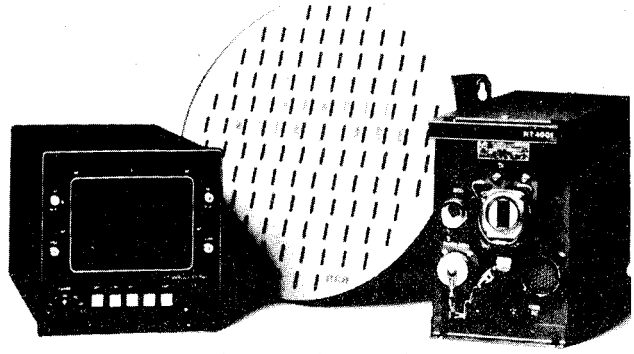

Fig. 5 RCA's Primus-400 weather radar (X-band).

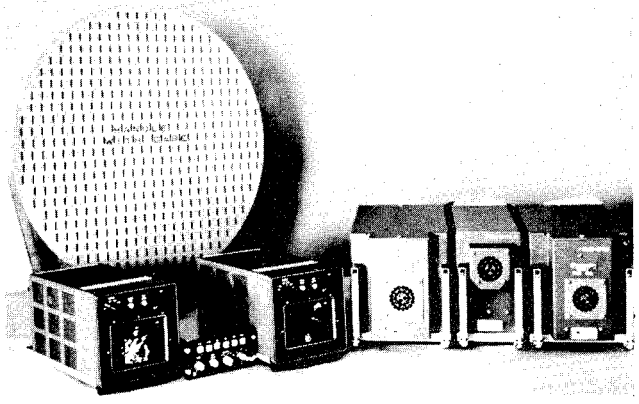

Fig. 6 RCA's multifunction weather radar display.

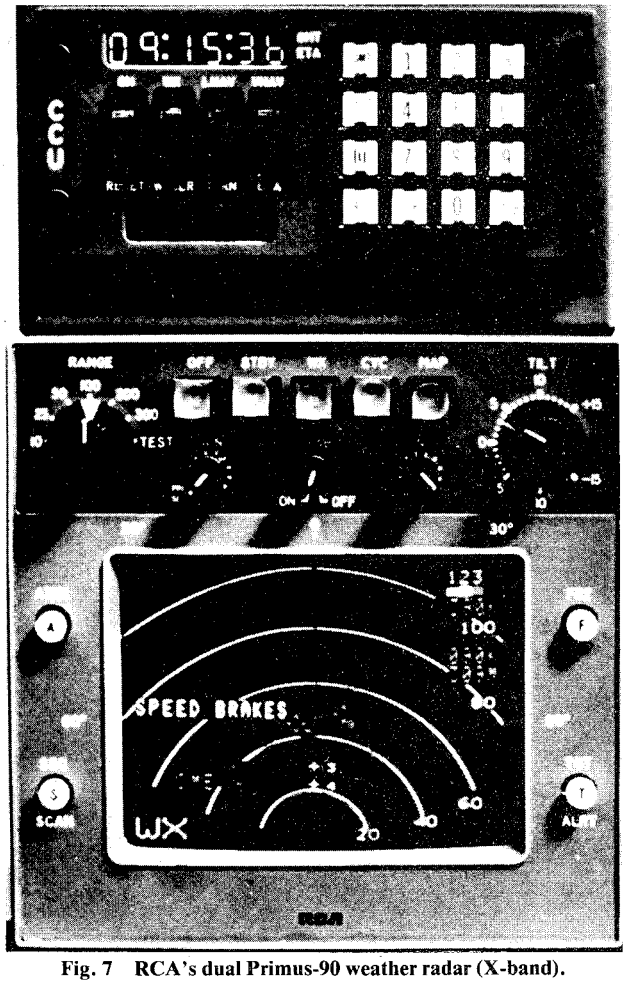

Fig. 7 RCA's dual Primus-90 weather radar (X-band).

Table 1 Comparison of the expected range performance for the new solid-state system and the high-powered magnetron systems range capability

	Magnetron systems, 60 kW		Solid-state system, 120 W
$P_t = 60$ kW	$P_t =$ 47.78 dB	$P_t = 120$ W	$P_t =$ 20.79 dB
$G = 34$ dB parabola	$2G =$ 68.0 dB	$G =$ 35-dB flate plate	$2G =$ 70.0 dB
$T = 2\ \mu$s	$2T =$ 6.0 dB	$T = 20\ \mu$s	$2T =$ 26.0 dB
$NF = 9$ dB (mixer)	$NF = -9.0$ dB	$NF = 5$ dB (GaAs FET)	$NF = -5.0$ dB
$B_f = 5 \log[(2 \times 1)/1.5]$	$B_f = -0.62$ dB		$B_f =$ 0.0 dB
$I = 3 \log[(3 \times 200)/180]$	$I =$ 1.57 dB	$I = 3 \log[(3 \times 240)/180]$	$I =$ 1.8 dB
$K =$ avoidance	6.0 dB	$K =$ avoidance	6.0 dB
	PI = 119.73 dB		PI = 119.59 dB
$R = \text{antilog}\frac{119.73 - 20}{40}$	= 311.35 miles	$R = \text{antilog}\frac{119.59 - 20}{40}$	= 308.85 dB

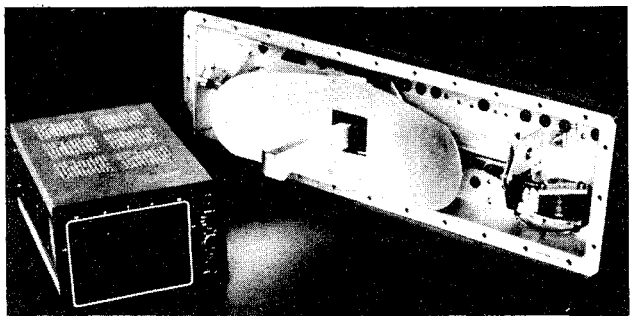

Fig. 8 RCA's weather Scout 1 single-engine aircraft weather radar (X-band).

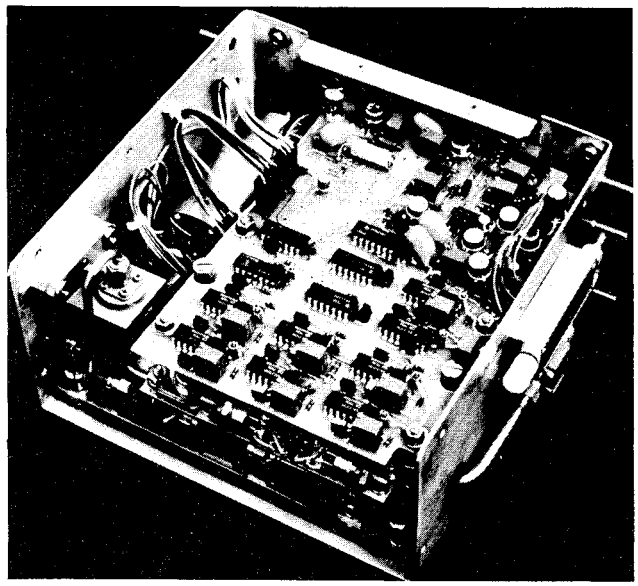

Fig. 9 100-W X-band multi-IMPATT cavity transmitter/modulator.

less than 35 lb, used solid-state modulators, generated less than 10 kW peak transmitter power, and employed pulse widths of greater than 2 μs (see Fig. 3). However, the airline industry continued to insist on high-powered (65 kW or more) C- or X-band transmitters with pulse widths of up to 6 μs with range capabilities of 300 n.mi. primarily to satisfy the then future needs for SST aircraft. These high-powered, heavy (125 lb), and power hungry (500 VA) systems are still produced for air-carrier use. This system is shown in Fig. 4.

It was not until 1974, when digital memory technology reached the point where the entire PPI radar display could be stored in high-speed 32 K ($128^2 \times 2$) memory for at least a 50 Hz refresh rate, that the industry took off in the new digital radar which resulted in the introduction of many other radar related innovations. The original Rho Theta display scan format used in the first digital display systems was soon replaced by a raster scan through the introduction of a solid-state converter. After the scan converter was designed and made cost effective, the system resolution was increased four-fold over earlier equipments by increasing the display memory to 131 K ($256 \times 256 \times 2$), and shortly thereafter this concept was applied to a shadow-mask-type color cathode ray tube (CRT) with the capability of displaying at least four colors using two planes of digital memory. Figure 5 shows a general aviation color radar system. This is the current state-of-the-art in display technology today except that three planes of memory systems are being introduced that are capable of simultaneously displaying eight colors.

The digital radar revolution of the mid 1970s carried along with it some other radar side effects. It provided the pilot with a nonflicker, nonfading colored display which is easy to interpret and view in normal cockpit lighting. In addition, alphanumerics can be displayed, thus providing the pilot with more information at a glance. Postdetection correlation schemes for signal-to-noise (S/N) improvement were introduced, further reducing the need for high-powered radar systems to achieve adequate radar range. Navigation tracks, checklists, and other pictorial information is now being shown on radar indicators along with weather. Figure 6 shows an airline X-band dual system and Fig. 7 is a multifunction display radar indicator.

General aviation weather radar systems are being produced today with peak transmitter power levels of 1 kW, pulse widths of up to 10 μs, display range scales of up to 200 n.mi., requiring 50 W of 28 V power, and weighing approximately 15 lb. This technology has made it possible to design a weather radar system for single engine aircraft where this radar is installed in the leading edge of the wing (see Fig. 8). As a result, there is practically no powered aircraft which cannot find a weather radar suitable for their needs. Helicopters have been using weather radar systems (some with beacon capability) for many years for both weather detection and as an aid in navigation, especially in those areas off the coast where oil platforms are located.

Using the airline industry weather radar range equation,† it has been determined that a current technology solid-state transmitter weather radar can be designed to provide adequate weather range detection for weather avoidance flying. The state-of-the-art (suitable to airline economy) will permit the development of about 120 W of peak power using many GaAs or Si IMPATTS (impact avalanche transit time diodes) combined in a cavity or by developing greater than 1 kW of power from transistors at close to 1 GHz and then multiplying the output to X-band using many varactors.

†The derivation of this equation is contained in the Appendix.

Radars using both of these solid-state transmitter concepts are already flying. Figure 9 shows a 100-W solid-state X-band transmitter. The reason for pursuing the development of solid-state transmitters is to improve equipment reliability, which is very important to the airlines. With the performance index (PI) and range equation developed in the Appendix, a comparison of the expected range performance for the new solid-state system and the high-powered magnetron systems range capability is compared in Table 1.

It is obvious that a properly designed 120-W solid-state transmitter weather radar can provide the same detection range as a 60-kW magnetron radar currently used in the airline industry. Because storm cells are generally relatively large, it is possible to consider employing long transmitter pulses. When the radar is adjusted for long ranges, the 20-μs resolution is acceptable. For example, with a radar system whose display resolution is limited by 256 range bins for a 300-mile range scale, each range bin is 300/256 or a 1.1718-mile range while the 20 μs yields a radar range resolution of 1.619 miles. For shorter ranges, where higher target resolution is desired, the transmitter pulse width can be made shorter while the receiver bandwidth is made wider, so as to retain a relatively close relationship between the display resolution and the range resolution.

Coherent (Doppler) Weather Radar Systems of the Future

The airline industry has requested that the radar manufacturers develop highly reliable solid-state weather radars. As a result, ARINC Characteristics 708 was prepared to standardize the radar configuration and digital signal interface so that many manufacturers may produce interchangeable systems. A solid-state weather radar designed to this characteristic is shown in Fig. 10. These new solid-state radars are being specified for new Boeing, Douglas, and Lockheed aircraft domestically. Some airlines are planning to retrofit these new radars into older aircraft.

Airborne weather radar systems used by the air-carrier and general aviation industry have been designed to process only the echo power or zero moment of the Doppler spectrum of the radar backscatter, which is an indication of the liquid water content or precipitation rate in the resolution volume. With the advent of low-powered solid-state Doppler weather radar systems, in addition to the zeroth moment, these new radar systems will have the capability of extracting the mean Doppler velocity or the first moment of the spectrum normalized to the zeroth moment, which for all practical airborne applications is the rain impregnated air motion towards or away from the radar, and the extraction of the spectrum width, which is the square root of the second moment about the first moment, which is a measure of the velocity dispersion (a direct measurement of turbulence), again, within the resolution volume of the radar.

Doppler weather radar designers are bound by many restraints not experienced with the non-Doppler radars currently being used. As a result, many tradeoffs must be made. A discussion of the tradeoffs, potential problems, possible solutions, and signal processing for these new airborne Doppler weather radar follows. A block diagram of the weather Doppler radar receiver is shown in Fig. 11.

The added complexity of the Doppler over the weather intensity measuring systems in use today consists of 1) a coherent transmitter-receiver in order to maintain phase coherency to extract the spectrum signal components; 2) the addition of a received signal quadrature phase separator along with the appropriate analog-to-digital (A/D) converter; 3) an accurate AGC circuit (based on radar return signals, not only noise); and 4) a high-speed real-time spectrum signal processor (FFT or complex covariance calculator) to extract the first and preferably the second Doppler moment. The design details to accomplish these functions are beyond the scope of this paper.

Because it is desirable to minimize the resolution volume so as to better define localized shear and other turbulence cell velocities, it is necessary to maintain the antenna beam width as narrow as possible. Most wide-body and current air-carrier aircraft are configured to accept up to a 30-in. (76-cm) diam circular aperture antenna which yields a 3-dB beam width of approximately 3 deg at X-band and 5 deg at C-band. As a result, the industry has tended towards the use of X-band for their weather radar needs since the primary mode of operation is weather avoidance. Transmitter pulse widths of up to 2 μs have been used on ground-based S-band Doppler radars with some success; however, it may be necessary to employ considerably wider pulse widths for airborne systems in order to realize adequate S/N and sensitivity to detect low reflectivity targets at reasonable ranges. This is one of the design tradeoffs which must be considered.

When the pulsed radar pulsed repetition frequency (PRF) is increased to the relatively high values necessary to extract the velocity spectrum widths of the echos at a particular range, consideration must be given to echos from other trips at $CT_s/2$ intervals which cause range aliasing and can prevent distinguishing between real Doppler shifts and those from aliased spaced frequency. The theoretical range velocity

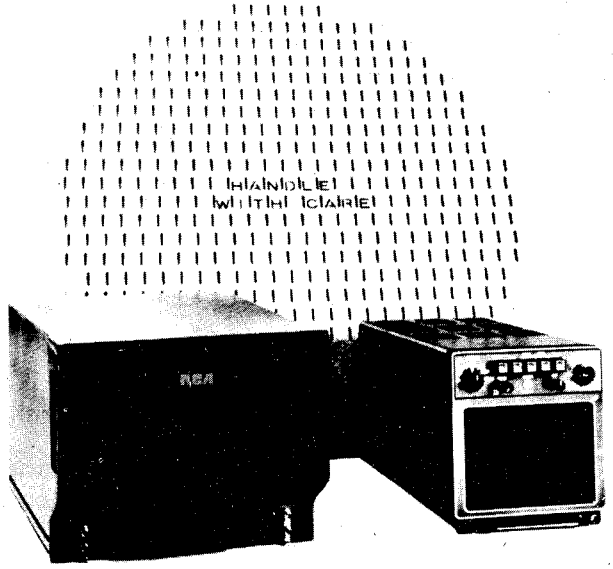

Fig. 10 Experimental RCA Primus-708 weather radar (X-band).

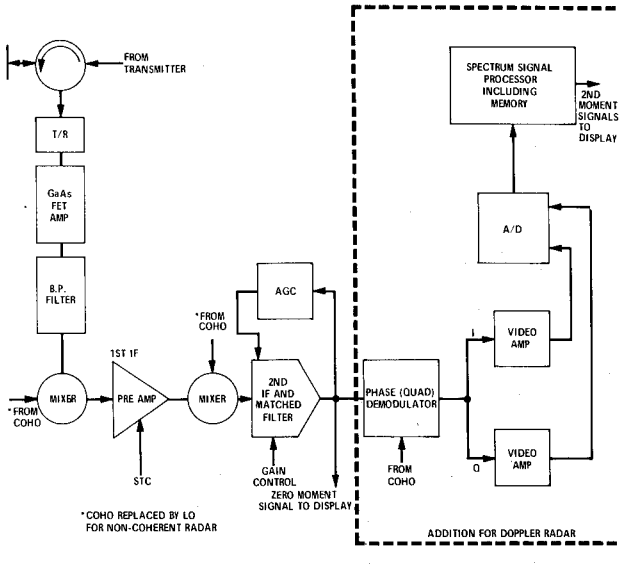

Fig. 11 Block diagram of a Doppler radar receiver.

product

$$r_a v_a = C\lambda/8$$

indicates the ambiguity resolution capabilities of a conventional uniformly pulse spaced Doppler radar.

If T_s is chosen large enough so as to avoid second or higher order trip echos from being received, then an examination of Nyquist interval $\lambda/2T_s$ is necessary to determine the expected σ_v. It has been shown that correlation exists when $\lambda/2T_s \gg \sigma_v$ (Ref. 1) where σ_v is the velocity spectrum width of the echo at range r. Since the Nyquist velocity v_a is $\pm\lambda/4T_s$, the maximum v_a for a reasonable range of 50-n.mi. radar operating at X-band is calculated as follows:

$$r_a = \frac{CT_s}{2} \qquad T_s = \frac{50 \times 1852 \times 2}{3 \times 10^8} = 6.17 \times 10^{-4}\ \mu s$$

$$v_a = \frac{\lambda}{4T_s} = \frac{0.032}{4 \times 6.17 \times 10^{-4}} = 12.966\ \text{m/s}$$

Velocity aliasing will occur if the spectrum width σ_v is anything but close to zero; therefore allowance must also be made for this fact, thus preventing accurate measurements to be made up to the 12.966 m/s calculated. In addition, analysis has shown that to maintain good signal sample correlation, the relationship $\lambda/2T_s > 2\pi\sigma_v$ applies.[1] This results in a spectrum width capability of 4.12 m/s for the X-band Doppler radar system which has an unambiguous range of 50 n.mi., the maximum range for this radar configuration. Consideration for a shorter unambiguous range to increase spectrum width measurements will only further aggravate the multiple trip problem.

The next issue has to do with methods which may be used to reduce the ambiguous range problem. Many complex and not adequately analyzed techniques which may apply to a commercial airborne weather radar system have been suggested, and some tried, which can extend the maximum unambiguous range and velocity measurements. A few which hold some promise are 1) random signal radar; 2) phase diversity; 3) spaced pulse pairs; 4) staggered PRT; and 5) dual-sampling techniques. The merits and disadvantages of these techniques are discussed in Ref. 1.

The minimum antenna scan rate acceptable to the airline industry is 45 deg/s (Ref. 2) so as to update the radar PPI at least 15 times per min for a 180-deg scanned forward sector. For a 3-deg beam width, the 3-dB antenna beam at this scan rate scans past a point target in 0.067 s and for a 1620 Hz PRF, 108 pulses can be processed. As a result, a practical real-time Doppler processor would be a 64-point FFT or 64 samples for a covariance or pulse-pair estimator. Either scheme should provide sufficient resolution to extract the second moment signals, provided that the spectrum width is no greater than the 0.4 of the Nyquist velocity. Regardless of the processing scheme used, it is desirable to work with S/N as high as 15 dB, as noted.[1]

Recognizing the above restraints, it appears that a significant reduction in the radar range detectability over current radars will result. First, it can be assumed that there is little need to examine the potential turbulence to be expected in a storm cell with a reflectivity factor Z or much greater than the 10^3. Aircraft are to avoid, by approximately 20 miles, storm cells with a reflectivity of $Z = 10^4$ owing to a relatively high probability of turbulence and some hail content. Therefore, if the radar range is to be predicted on a maximum reflectivity of $Z = 10^3$, and using a relatively wide pulse width, for example, of 6 μs, the maximum range is calculated to be approximately 50 miles.

$$\text{PI} = P_t + 2G + 2T - NF + I - B_f + K$$

$$= 20.79 + 70 + 15.56 - 5 + 4.29 + 6 = 111.64$$

PI is based on $Z = 10^5$. For $Z = 10^3$ intensity subtract 20 dB from the PI. The equation is based on a 11.5 dB S/N. For 15 dB S/N, therefore, subtract 3.5 dB. Therefore

$$\begin{aligned} \text{PI} = \ & 111.64\ \text{dB} \\ & -20.0\ \text{dB} \\ & -3.5\ \text{dB} \\ \hline & 88.14\ \text{dB} \end{aligned}$$

$$\text{Range} = \text{antilog}\frac{88.14 - 20}{40} = 50.52\ \text{n.mi.}$$

This is consistent with the expected Doppler range detection for a $Z = 10^3$ storm intensity and a 15 dB S/N. Lower reflectivity signals can be detected with a lower S/N. Note that the above PI applies to a nonbeam filling radar case where the storm cell diameter is 2.6 n.mi. or less—a practical condition. The intervening rain attenuation must not exceed 2.25 dB.

It is necessary to prevent ground clutter contamination of the weather backscatter signals to adequately assess potential storm cell turbulence. As a result, the new weather radar systems will employ high resolution digital stabilization signal processors to correctly solve the complex airborne stabilization equation so as to reduce the likelihood of terrain illumination. This places an added burden on the aircraft vertical stabilization sensors. In the past, vertical gyros were employed with their attendant processing problems. Inertial platforms have found their way into wide-bodied aircraft and it can be expected that more reliable and cost effective laser gyros (strap-down) will become common in the air-carrier aircraft of the future. Slotted array (flat-plate) radar antennas are becoming standard in these aircraft. Sidelobes of at least 25 dB down from the main lobe are produced with essentially no radiation off the ends of the arrays, thus significantly reducing the effect of terrain sidelobe clutter contamination. Even so, the industry is developing techniques to further reduce main-lobe clutter signals by video processing with the new coherent radar systems. Many schemes have been evaluated in the past, however, the best clutter suppressor is that which prevents the antenna from illuminating the terrain, and this can be accomplished by generating low sidelobes, providing accurate antenna stabilization, and using proper tilt management, whether it be automatic or manual.

Because the radar antenna scan rate is relatively fast and the aircraft is moving relative to both the storm cell and the terrain, at best, the ability to separate the ground or terrain clutter signature from the weather signals is proving to be difficult. Since the storm cell may not be moving relative to the terrain below, it is not always possible to reject one or the other by first moment processing since these signals fall in the same velocity cell. Therefore an MTI scheme may not always be practical. The clutter and weather spectrum signal signatures are usually different and can be further distorted by the antenna scan rate and aircraft velocity. Amplitude modulation backscatter scintillation frequencies are relatively low for terrain targets and much higher for meteorological signals. To separate these frequencies has not yet been proven acceptable owing to the fact that both signal frequencies overlap, thus much of the weather signature signals can be removed along with the clutter by the processor.

Because weather radars are designed and calibrated to detect and display rainfall rates (intensity), their use as a means for navigating through a storm cell is very restrictive. Dry hail, ice crystals, and snow radar backscatter coefficients differ significantly from that of uniform rainfall. As a result, these radars can only be relied on to display rainfall rates provided the intervening rain attenuation is insignificant.

A sensitivity time control (STC) feature is designed into most weather radars to maintain the same received signal level for the storm constant over a limited range, usually at a range starting where a 3-mile-diam cell just fills the antenna 3-dB

beam width. However, most radars do not sense the intervening rain or fog attenuation which may exist between the radar and the storm cell. Therefore the cell may appear considerably less intense than it actually is owing to the intervening signal attenuation environment. Designers are attempting to compensate for this attenuation by sampling the radar backscatter signals and then adjusting the receiver sensitivity accordingly for each sampled range and azimuth increment. However, clouds (heavy fog) whose water content particles are small compared to rain may attenuate radar signals significantly without producing a detectable signal at the radar. In this special case, there is no known solution to the radar signal attenuation compensation except to select a low radar carrier frequency (usually below 3 GHz) where the attenuation is insignificant.

Conclusions

The advent of new solid-state technology components has changed the airborne weather radar using World War II technology from a large, heavy, and power hungry system whose reliability was measured in hours to a relatively small, light-weight, low-powered, and highly reliable device. However, up to this time, the storm cell detection principle has not changed significantly; the radars are designed to detect rainfall rate only, and it is up to the user to assess the radar display to determine a turbulence-free path past the storm cell by avoiding the heavier rainfall areas and noting other turbulence signature signals either from experience or known meteorological phenomena. The user has not had available to him a display which provides storm cell turbulence locations or other related hazards to flying. High-speed low-cost digital technology has made it possible to produce flicker-free and nonfading color displays which can easily be viewed in normal cockpit light. This same digital technology may soon provide the user with more storm cell signature information which will promote flight safety when flying near known storms. Unnecessary course deviations can thereby be reduced, thus helping to conserve fuel. The introduction of solid-state transmitters will eventually provide for not only a reduction in cost of ownership, but for reduced maintenance time, thus helping to maintain schedules. Weather radar can be a useful tool for avoiding encounters with turbulent storm cells, but the pilot must be trained to be aware of its limitations.

Appendix

The radar range equation has been developed in many places and usually takes the form

$$R=\left(\frac{P_t G^2 \lambda^2 \sigma}{(4\pi)^3 P_r L}\right)^{1/4} \qquad \text{(A1)}$$

The value of σ, which is the radar target cross section in m^2, miles^2, or whatever terms being used in the equation when used for weather detection, is defined as

$$\sigma=(\pi^5/\lambda^4)\,|K|^2 Z \qquad \text{(target pulse volume)} \qquad \text{(A2)}$$

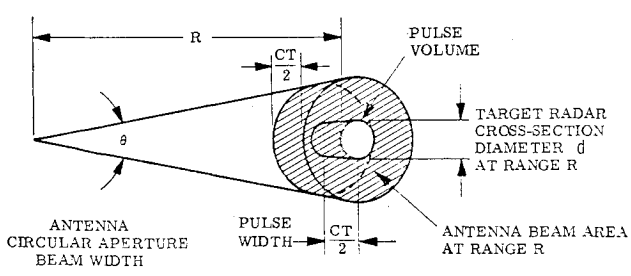

Fig. A1 Target pulse volume.

The target pulse volume is $(CT/2)(d^2/4)$ (see Fig. A1), where C is the speed of propagation, T is the transmitter pulse width, and d is the diameter of the storm cell.

Substituting Eq. (A2) into Eq. (A1), we obtain the meteorological radar range Eq. (A3):

$$R^4=\frac{P_t G^2 T}{P_r L \lambda^2}\left[\frac{\pi^3 d^2 Z C |K|^2}{512}\right]^{\ddagger} \qquad \text{(A3)}$$

Since the range equation will be expressed in nautical miles, transmitter power in watts, and transmitter pulse width in microseconds, it is necessary to convert the equation terms accordingly.

Conversion Calculations

$$C=\frac{3\times 10^8 \text{ m/s}}{1852 \text{ m/n.mi.}}=1.61987\times 10^5 \text{ n.mi./s}$$

$$T=10^{-6} \text{ s}/\mu\text{s}=10^{-6} \text{ s}$$

$$d=3 \text{ n.mi.}$$

$$d^2=9 \text{ (n.mi.)}^2$$

$$Z=10^5=1.5743\times 10^{-23} \text{ (n.mi.)}^3$$

$$\pi^3=31.0$$

$$|K|^2=0.93 \text{ (for all weather radar bands)}$$

$$P_r=KTB \text{ S/N } NF \qquad (KT=10^{-21} \text{ W/Hz bandwidth, } B=1/T)$$

$$\lambda^2 \text{ (X-band)}=\left(\frac{0.032 \text{ m}}{1852 \text{ m/n.mi.}}\right)^2=2.98564\times 10^{-10} \text{ (n.mi.)}^2$$

Equation (A3) is converted as follows:

$$R^4=\frac{P_t G^2 T^2}{NF \text{ S/N } L}\left[\frac{\pi^3 d^2 Z C |K|^2}{KT512\lambda^2}\right] \qquad \text{(A4)}$$

$$=\frac{P_t G^2 T^2}{NF \text{ S/N } L}\left[\frac{10^{-12}\times 31\times 9\times 1.5743\times 10^{-23}}{10^{-21}\times 512\times 2.9856\times 10^{-10}} \times 1.6198\times 10^5\times 0.93\right]$$

$$R^4=\frac{P_t G^2 T^2}{NF \text{ S/N } L}(4.32847) \qquad \text{(A5)}$$

Converted to dB format,

$$40\log R=10\log P_t+20\log G+20\log T - 10\log NF-10\log \text{S/N}-10\log L+10\log 4.32847$$

In abbreviated form,

$$40\log R=P_t+2G+2T-NF-\text{S/N}-L+6.35 \text{ (dB)} \qquad \text{(A6)}$$

A S/N (single pulse) of 11.5 dB has been assumed,

$$P_{fa}=10^{-6} \qquad P_d=50\%$$

Installation losses have been estimated to be 7 dB.

Intervening rain attenuation for avoidance calculations has been assumed to be at a rainfall rate of 1 mm/h over a 60-mile

‡$\ell n 2$ in the denominator is sometimes used.

range [0.0375dB/n.mi. (X-band) × 60 miles = 2.25 dB].

The total losses follow:

11.5 dB	S/N
7.0 dB	installation
2.25 dB	intervening rain
20.75 dB	≃ 20 dB

The 6.35-dB factor in Eq. (A6) has been rounded off to 6 dB at X-band and defined as a K factor.

The range equation (A6) becomes

$$40\log R = P_t + 2G + 2T - NF + K - 20\,(\text{dB}) \qquad \text{(A7)}$$

There have been some different approaches used to establish this equation in the past; however, the end result is essentially the same.

In order to account for a mismatch between the transmitted pulse width and the receiver bandwidth, a bandwidth factor penalty according to the following equation will be assessed (empirically derived).

$$B_f = 5\log(BT/1.5)$$

where B is the receiver bandwidth and T is the transmitter pulse width.

In addition, a postdetection correlation factor I has been added to provide for S/N improvement if more than one pulse is used for correlation purposes.

$$I = 3\log\frac{\text{PRF(Hz)} \times \text{antenna beam width (deg)}}{\text{total antenna scan angle (deg)}}$$

The final form of the weather radar range equation becomes

$$40\log R = P_t + 2G + 2T - NF + I - BF + K - 20\,(\text{dB}) \qquad \text{(A8)}$$

defining PI as

$$P_t + 2G + 2T - NF + I - B_f + K\,(\text{dB}) \qquad \text{(A9)}$$

$$\text{range} = \text{antilog}\frac{\text{PI} - 20}{40}\ \text{n.mi.} \qquad \text{(A10)}$$

This equation may be found in ARINC Characteristics 564 and ARINC Characteristics 708, and the PI formula (A9) may be found in RTCA Document DO-134.

It is known as the radar weather avoidance case for X-band when the total installation losses amount to 7 dB. For other values of installation losses, such as short antenna transmission runs, good radomes, etc., appropriate changes to the 7 dB are permitted.

The air-carrier industry has defined the weather penetration environment as consisting of a uniform 5-mm/h rainfall rate over a range of 60 n.mi. Using empirically derived and published attenuation values for this intervening rain condition, the K factor for the X-band radar is −6 dB. For the C-band radar system the avoidance K factor is listed as +3 dB and the penetration factor as 0 dB. Due to the excessive attenuation for Ku-band signals, this frequency radar has not beeen developed recently.

References

[1] Doviak, R.J., Zrnik, D.S., and Sirmans, D.S., "Doppler Weather Radar," *Proceedings of the IEEE,* Vol. 67, No. 11, Nov. 1979, pp. 1522-1553.

[2] ARINC Characteristics 708, "Airborne Weather Radar," Aeronautical Radio, Inc., Md., Dec. 21, 1979.